Variable structure attitude control for a rolling aerial vehicle via extended state observer

Qi Chen
School of Energy and Power Engineering
Nanjing University of Science and Technology
Nanjign, China
qiychan@126.com

Xing-Gang Yan
School of Engineering and Digital Arts
University of Kent
Kent, United Kingdom
x.yan@kent.ac.uk

Zhongyuan Wang
School of Energy and Power Engineering
Nanjing University of Science and Technology
Nanjign, China
zywang@njust.edu.cn

Jianqiu Mu
School of Engineering and Digital Arts
University of Kent
Kent, United Kingdom
jm838@kent.ac.uk

***Abstract* — A novel attitude control scheme is proposed for a rolling aerial vehicle (RAV) with large uncertainties. Firstly, the RAV highly coupled nonlinear system is separated into attitude loop and angular loop via backstepping technique. The nominal states are calculated based on the procedure of trajectory linearization control (TLC). Then, extended state observers (ESO) are applied to estimate the uncertainties in the RAV system. Meanwhile, a feedback linearization-based controller is synthesized for the attitude loop using the estimated uncertainties, and an ESO-based sliding mode controller is synthesized for the angular rate loop. The stability of the closed-loop system is studied. Simulation results with comparisons are presented to demonstrate the feasibility of the proposed control scheme.**

Keywords* — *Rolling aerial vehicle, backstepping control, extended state observer, variable structure control.

I. INTRODUCTION

A rolling aerial vehicle (RAV) is a kind of aerodynamic controlled missile and flies with a sustained roll rate which is mainly produced by a set of oblique fins. The RAV has advantages of small volume, inherent capacity of compensating for thrust asymmetries and fin misalignments. In addition, low requirement for flight control gyros, accelerometers, and actuators results in a relatively low cost for RAV. These advantages make this kind of vehicles become attractive and promising in military situations [1-3]. However, due to the rolling motion, the dynamics of pitch and yaw channels can be highly coupled with each other, which makes the attitude control design intractable. It is difficult for traditional control design scheme based on each independent channel to achieve a satisfactory performance. Therefore, there is a need to develop an integrated attitude control law using modern advanced control techniques.

In recent years, much research have been carried out on attitude control and many control approaches have been proposed. An adaptive backstepping approach was presented in [4], where a wide range of flight envelope is considered, but only the longitudinal dynamic model is taken into account. In [5], Parker et al proposed a nonlinear control method combining an inner loop feedback linearization and an outer loop LQR controller with integral augmentation. This method has shown good robustness with respect to small parameter variations. To further increase the robustness, a robust nonlinear tracking controller by using a min-max LQR control approach was proposed in [6,7]. This controller provides robust stability and good performance for the systems under varying flight conditions. Trajectory linearization control (TLC) has been proven to be an alternative approach for nonlinear tracking problems. It combines an open-loop nominal system and a linear time-varying feedback linearization stabilization, and can provide a certain extent of rejecting disturbances [8,9]. Since only linear term of the original nonlinear system is reserved, this method can only achieve local results. To increase the robustness of TLC in absence of large uncertainties, adaptive neural network was adopted to approximate the uncertainties online [10]. However, due to the complexity of this theory, how to tune the corresponding parameters is a great challenge.

Although the approaches mentioned above have achieved satisfactory performance, but none of them is concerned with the RAV system with highly coupled nonlinear dynamics. Variable structure control has high robustness against uncertainties and can be used to deal with both matched and mismatched uncertainties [14,15,16]. By combining variable structure control and the approaches mentioned above, the attitude control problem for the RAV is considered in this paper. Using backstepping technique and the framework of TLC, extended state observers (ESO) and the observer-based variable structure controllers are developed to tackle the large uncertainties to further improve the performance of the closed-loop system. Simulation and comparison are further presented to demonstrate the effectiveness of the proposed approach.

II. NONLINEAR ATTITUDE DYNAMICS OF RAV

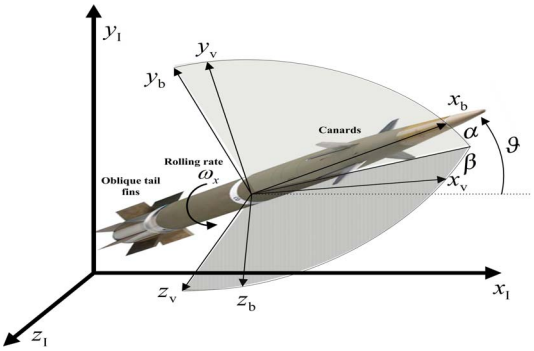

Fig. 1 RAV configuration and reference frames

Figure 1 illustrates the vehicle's configuration and the reference frames: x_I-y_I-z_I represents the inertial reference frame, x_b-y_b-z_b and x_v-y_v-z_v represent the body-fixed and velocity-fixed reference frames respectively. The variables α, β are angle of attack and sideslip angle respectively, which represent the relation between x_b-y_b-z_b and x_v-y_v-z_v. The variable ϑ is the pitch angle. RAV dynamics are usually modeled as a six-degree-of – freedom (6-DOF) motion which consists of translational motion and rotational motion. The translational motion is mainly used to describe the behavior of the center-of-mass, while the rotational motion is used to describe the behavior of the vehicle around its center-of-mass. This work only focuses on the attitude control of the RAV, the equations of translational motion are not considered. The rotational motion governing the rigid-body attitude dynamics of the RAV, can be described by the following equations (see, [11])

$$\begin{cases} \dot{\alpha} = -F_{ya}/(mV\cos\beta) - \omega_y\cos\alpha\tan\beta\tan\vartheta + \omega_y\sin\alpha\tan\beta + \omega_z \\ \dot{\beta} = F_{za}/mV + \omega_y\sin\alpha\tan\vartheta + \omega_y\cos\alpha \\ \dot{\omega}_z = M_z/J_z + J_x\omega_y\omega_x/J_z - J_y\omega_y^2\tan\vartheta/J_z \\ \dot{\omega}_y = M_y/J_y - J_x\omega_x\omega_z/J_y + J_z\omega_z\omega_y\tan\vartheta/J_y \end{cases} \tag{1}$$

where

$$\begin{bmatrix} F_{ya} \\ F_{za} \end{bmatrix} = \frac{1}{2}\rho V^2 S_{ref} \times \begin{bmatrix} c_y \\ c_z \end{bmatrix} + \begin{bmatrix} -mg\cos\theta\cos\gamma_v \\ mg\cos\theta\sin\gamma_v \end{bmatrix}$$

$$= \frac{1}{2}\rho V^2 S_{ref} \times \begin{bmatrix} c_y^{\alpha}\alpha + c_y^{\delta_z}\delta_z \\ c_y^{\beta}\beta + c_y^{\delta_y}\delta_y \end{bmatrix} + \begin{bmatrix} -mg\cos\theta\cos\gamma_v \\ mg\cos\theta\sin\gamma_v \end{bmatrix}$$

$$\begin{bmatrix} M_y \\ M_z \end{bmatrix} = \frac{1}{2}\rho V^2 S_{ref} l \times \begin{bmatrix} m_y \\ m_z \end{bmatrix}$$

$$= \frac{1}{2}\rho V^2 S_{ref} l \times \begin{bmatrix} m_z^{\alpha}\alpha + m_z^{\bar{\omega}_z}\dfrac{\omega_z l}{V} + m_z^{\delta_z}\delta_z \\ m_y^{\beta}\beta + m_y^{\bar{\omega}_y}\dfrac{\omega_y l}{V} + m_y^{\delta_y}\delta_y \end{bmatrix}$$

where $\dot{\vartheta} = \omega_z$, the symbols ω_x, ω_y, ω_z are rolling rate, yawing rate, and pitching angular rate respectively, δ_y and δ_z denote the equivalent rudder and elevator deflections, which are the control variables, c_y and c_z are lift and lateral force coefficients, m_y and m_z are yawing and pitching moment coefficients respectively. The other parameters can be referred to [11]. As it is assumed that the RAV is equipped with oblique fins and flying with an approximated constant roll rate, the roll angular rate ω_x is considered as a constant and thus the rolling dynamics can be neglected. Clearly, the presence of ω_x increases the coupling between the yaw and the pitch.

It is noted that the aerodynamic forces generated by the deflections δ_y and δ_z are negligible. Assuming that the flight path angle is known, the gravity can be compensated in advance. Therefore, the model (1) can be slightly simplified. For simplicity, the following parameters are introduced

$$a_{34} = \frac{\rho V^2 S_{ref} c_y^{\alpha}}{2mV},\ b_{34} = \frac{\rho V^2 S_{ref} c_z^{\beta}}{2mV},\ a_{24} = \frac{\rho V^2 S_{ref} l m_z^{\alpha}}{2J_z},$$

$$b_{24} = \frac{\rho V^2 S_{ref} l m_y^{\beta^*}}{2J_y},\ a_{22} = \frac{\rho V^2 S_{ref} l^2 m_z^{\bar{\omega}_z}}{2VJ_z},\ b_{22} = \frac{\rho V^2 S_{ref} l^2 m_y^{\bar{\omega}_y}}{2VJ_y},$$

$$a_{25} = \frac{\rho V^2 S_{ref} l m_z^{\delta_z}}{J_z},\ b_{25} = \frac{\rho V^2 S_{ref} l m_y^{\delta_y}}{J_y},\ c_1 = \frac{J_x\omega_x}{J_z},\ c_2 = \frac{J_x\omega_x}{J_y}$$

System (1) can be rewritten in the following compact form as

$$\dot{\mathbf{X}}_1 = \mathbf{F}_1(\mathbf{X}_1) + \mathbf{B}_1(\mathbf{X}_1)\mathbf{X}_2 + \Delta\mathbf{d}_1 \tag{2}$$

$$\dot{\mathbf{X}}_2 = \mathbf{F}_2(\mathbf{X}_1, \mathbf{X}_2) + \mathbf{B}_2(\mathbf{X}_1)\mathbf{U} + \Delta\mathbf{d}_2 \tag{3}$$

where

$$\mathbf{X}_1 = \begin{bmatrix} \alpha \\ \beta \end{bmatrix},\ \mathbf{X}_2 = \begin{bmatrix} \omega_z \\ \omega_y \end{bmatrix},\ \mathbf{U} = \begin{bmatrix} \delta_z \\ \delta_y \end{bmatrix},\ \mathbf{F}_1(\mathbf{X}_1) = \begin{bmatrix} -a_{34}\alpha \\ -b_{34}\beta \end{bmatrix} \tag{4}$$

$$\mathbf{B}_1(\mathbf{X}_1) = \begin{bmatrix} 1 & -\cos\alpha\tan\beta\tan\vartheta + \sin\alpha\tan\beta \\ 0 & \sin\alpha\tan\vartheta + \cos\alpha \end{bmatrix} \tag{5}$$

$$\mathbf{F}_2(\mathbf{X}_1, \mathbf{X}_2) = \begin{bmatrix} a_{24}\alpha + a_{22}\omega_z + c_1\omega_y - \omega_y^2\tan\vartheta \\ b_{24}\beta + b_{22}\omega_y - c_2\omega_z + \omega_z\omega_y\tan\vartheta \end{bmatrix} \tag{6}$$

$$\mathbf{B}_2(\mathbf{X}_1) = \begin{bmatrix} a_{25} & 0 \\ 0 & b_{25} \end{bmatrix} \tag{7}$$

The symbols $\Delta\mathbf{d}_1$ and $\Delta\mathbf{d}_2$ include all the modeling errors and disturbances existing in the RAV. It is assumed that there exist positive constants $d_{1\max}$, $d_{2\max}$ such that $\Delta\mathbf{d}_1$ and $\Delta\mathbf{d}_2$ satisfy

$$\|\Delta\mathbf{d}_1\| \le d_{1\max},\ \|\Delta\mathbf{d}_2\| \le d_{2\max}.$$

The objective of this paper is to design a control law $\mathbf{U} = \begin{bmatrix} \delta_z & \delta_y \end{bmatrix}^T$ for the RAV described in Eqs. (2) and (3), such that the output $\mathbf{X}_1 = \begin{bmatrix} \alpha & \beta \end{bmatrix}^T$ tracks the pre-given reference command $\mathbf{X}_1^{\text{ref}}(t) = \begin{bmatrix} \alpha_{\text{ref}}(t) & \beta_{\text{ref}}(t) \end{bmatrix}^T$ even in the presence of modelling errors and external disturbances.

III. NONLINEAR CONTROL LAW DESIGN

It should be noted that Eqs. (2) and (3) have special structure, which makes the backstepping method applicable. By using backstepping method, the RAV system can be decomposed into an attitude loop subsystem and angular rate loop subsystem. Fig. 2 shows the control architecture for RAV.

The attitude loop is used to track the reference command $\mathbf{X}_1^{\text{ref}}(t)$ by considering the angular rate $\mathbf{X}_2$ as the virtual input, whereas the angular rate loop is employed to regulate the

angular rate by designing the actual control input $\mathbf{U}$ so that the angular rate $\mathbf{X}_2$ tracks the reference angular rate $\mathbf{X}_2^{\mathrm{ref}}(t)$.

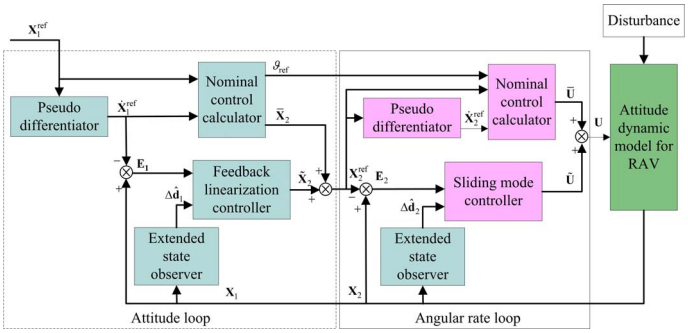

Fig. 2 The structure of the proposed control strategy for RAV

A. Control design for attitude loop

Based on the attitude loop subsystem and the design principle of TLC, the nominal virtual control $\bar{\mathbf{X}}_2$ (i.e. nominal angular rate) can be calculated and described by using Eq. (2) and the reference command $\mathbf{X}_1^{\mathrm{ref}}$

$$\bar{\mathbf{X}}_2 = \mathbf{B}_1(\mathbf{X}_1^{\mathrm{ref}})^{-1}(\dot{\mathbf{X}}_1^{\mathrm{ref}} - \mathbf{F}_1(\mathbf{X}_1^{\mathrm{ref}})) \tag{8}$$

where $\dot{\mathbf{X}}_1^{\mathrm{ref}}$ denotes the derivative of $\mathbf{X}_1^{\mathrm{ref}}$ and can be obtained by passing through a pseudo differentiator represented by the following transfer function [13]

$$G(s) = \frac{\omega_d s}{s + \omega_d} \tag{9}$$

where ω_d is the bandwidth of the pseudo differentiator.

Remark 1. According to the definition of $\mathbf{B}_1(\cdot)$ in (5), it can be obtained that

$$\begin{aligned}\det(\mathbf{B}_1(\mathbf{X}_1)) &= \left\| \begin{bmatrix} 1 & -\cos\alpha\tan\beta\tan\vartheta + \sin\alpha\tan\beta \\ 0 & \sin\alpha\tan\vartheta + \cos\alpha \end{bmatrix} \right\| \\ &= \sin\alpha\tan\vartheta + \cos\alpha \\ &= \cos(\vartheta-\alpha)/\cos\vartheta\end{aligned}$$

Note that $\vartheta - \alpha$ is approximately equal to the flight path angle and during the entire flight of RAV, ϑ and α belong to the following set

$$\left\{ (\vartheta,\alpha) \middle| |\vartheta-\alpha| < \frac{\pi}{2}, |\vartheta| < \frac{\pi}{2} \right\}$$

Therefore $\det\left(\mathbf{B}_1(\mathbf{X}_1^{\mathrm{ref}})\right) \neq 0$ can be guaranteed, i.e. the matrix $\mathbf{B}_1(\mathbf{X}_1^{\mathrm{ref}})$ is invertible.

Defining the tracking error $\mathbf{E}_1 = \mathbf{X}_1 - \mathbf{X}_1^{\mathrm{ref}}$ for the attitude loop subsystem, together with Eq. (2) and Eq. (8), the tracking error dynamics are formulated as

$$\begin{aligned}\dot{\mathbf{E}}_1 &= \dot{\mathbf{X}}_1 - \dot{\mathbf{X}}_1^{\mathrm{ref}} = \mathbf{F}_1(\mathbf{X}_1) + \mathbf{B}_1(\mathbf{X}_1)\mathbf{X}_2 + \Delta\mathbf{d}_1 - \mathbf{F}_1(\mathbf{X}_1^{\mathrm{ref}}) - \mathbf{B}_1(\mathbf{X}_1^{\mathrm{ref}})\bar{\mathbf{X}}_2 \\ &= \mathbf{F}_1(\mathbf{X}_1^{\mathrm{ref}} + \mathbf{E}_1) + \mathbf{B}_1(\mathbf{X}_1^{\mathrm{ref}} + \mathbf{E}_1)(\bar{\mathbf{X}}_2 + \tilde{\mathbf{X}}_2) + \Delta\mathbf{d}_1 - \mathbf{F}_1(\mathbf{X}_1^{\mathrm{ref}}) - \mathbf{B}_1(\mathbf{X}_1^{\mathrm{ref}})\bar{\mathbf{X}}_2\end{aligned} \tag{10}$$

where $\tilde{\mathbf{X}}_2 = \mathbf{X}_2 - \bar{\mathbf{X}}_2$. By linearizing (10) along the nominal trajectory ($\mathbf{X}_1^{\mathrm{ref}}$, $\bar{\mathbf{X}}_2$), it is obtained that

$$\dot{\mathbf{E}}_1 = \mathbf{A}_1(t)\mathbf{E}_1 + \mathbf{B}_1(t)\tilde{\mathbf{X}}_2 + \Delta\mathbf{d}_1 \tag{11}$$

where

$$\mathbf{A}_1(t) = \left(\frac{\partial \mathbf{F}_1(\mathbf{X}_1)}{\partial \mathbf{X}_1} + \frac{\partial(\mathbf{B}_1(\mathbf{X}_1)\mathbf{X}_2)}{\partial \mathbf{X}_1} \right)\Bigg|_{(\mathbf{X}_1^{\mathrm{ref}}, \bar{\mathbf{X}}_2)}, \quad \mathbf{B}_1(t) = \mathbf{B}_1(\mathbf{X}_1)\big|_{(\mathbf{X}_1^{\mathrm{ref}}, \bar{\mathbf{X}}_2)}.$$

In (11), $\tilde{\mathbf{X}}_2$ is viewed as a virtual control and designed as

$$\tilde{\mathbf{X}}_2 = \mathbf{B}_1(t)^{-1}\left[(\mathbf{K}_1 - \mathbf{A}_1(t))\mathbf{E}_1 - \Delta\mathbf{d}_1\right], \mathbf{K}_1 = \mathrm{diag}(k_{11}, k_{12}) \tag{12}$$

where $\mathbf{K}_1$ is a design matrix with $k_{11} > 0, k_{12} > 0$ to ensure the asymptotic stability of (11). It is noted that the virtual control (12) involves the uncertainty $\Delta\mathbf{d}_1$ which is completely unknown. In order to deal with this issue, a second-order ESO proposed in [12] is applied to estimate $\Delta\mathbf{d}_1$. Firstly, an extended state $\mathbf{X}_3$ is added as the uncertainty $\Delta\mathbf{d}_1$, and (2) can be rewritten as

$$\begin{cases} \dot{\mathbf{X}}_1 = \mathbf{F}_1(\mathbf{X}_1) + \mathbf{B}_1(\mathbf{X}_1)(\bar{\mathbf{X}}_2 + \tilde{\mathbf{X}}_2) + \mathbf{X}_3 \\ \dot{\mathbf{X}}_3 = \xi_1(t) \end{cases} \tag{13}$$

where the function $\xi_1(t)$ is the derivative of the uncertainty $\Delta\mathbf{d}_1$. Then the following ESO is constructed.

$$\begin{cases} \dot{\hat{\mathbf{X}}}_1 = \hat{\mathbf{X}}_3 + l_1\mathbf{e}_1 + \mathbf{F}_1(\hat{\mathbf{X}}_1) + \mathbf{B}_1(\hat{\mathbf{X}}_1)(\bar{\mathbf{X}}_2 + \tilde{\mathbf{X}}_2) \\ \dot{\hat{\mathbf{X}}}_3 = l_2\mathbf{e}_1 \end{cases} \tag{14}$$

where $\mathbf{e}_1 = \mathbf{X}_1 - \hat{\mathbf{X}}_1$ is the estimation error of the ESO, $\hat{\mathbf{X}}_1$ is the estimate of $\mathbf{X}_1$, $\hat{\mathbf{X}}_3$ is the estimate of $\mathbf{X}_3$ (i.e. the uncertainty $\Delta\mathbf{d}_1$), l_1 and l_2 denote the observer gains and are tuned by using bandwidth-based method [13]. The stability and convergence of ESO can be referred to [12,13]. Based on the estimated uncertainty $\hat{\mathbf{X}}_3$, the virtual control is modified as

$$\tilde{\mathbf{X}}_2 = \mathbf{B}_1(t)^{-1}\left[-(\mathbf{K}_1 + \mathbf{A}_1(t))\mathbf{E}_1 - \hat{\mathbf{X}}_3\right], \ \mathbf{K}_1 = \mathrm{diag}(k_{11}, k_{12}) \tag{15}$$

Then, from (8) and (15), the compound control law for attitude loop is designed as

$$\mathbf{X}_2^{\mathrm{ref}} = \bar{\mathbf{X}}_2 + \tilde{\mathbf{X}}_2 \tag{16}$$

where $\mathbf{X}_2^{\mathrm{ref}}$ denotes reference command for angular rate loop.

B. Control design for angular rate loop

Since the reference command for angular rate loop has been obtained in (16) in the previous section, following the process of TLC, the corresponding control for nominal system in (3) can be calculated as follows

$$\bar{\mathbf{U}} = \mathbf{B}_2(\mathbf{X}_1^{\mathrm{ref}})^{-1}\left(\dot{\mathbf{X}}_2^{\mathrm{ref}} - \mathbf{F}_2(\mathbf{X}_1^{\mathrm{ref}}, \mathbf{X}_2^{\mathrm{ref}})\right) \tag{17}$$

where $\bar{\mathbf{U}}$ is the nominal control (i.e. nominal rudder and elevator deflections) for angular rate loop. $\dot{\mathbf{X}}_2^{\mathrm{ref}}$ denotes the derivative of $\mathbf{X}_2^{\mathrm{ref}}$ and can be obtained by the pseudo differentiator (9). Similar to the process in section above, define the angular rate tracking error $\mathbf{E}_2 = \mathbf{X}_2 - \mathbf{X}_2^{\mathrm{ref}}$, the tracking error dynamics for angular rate system can be formulated as

$$\begin{aligned}\dot{\mathbf{E}}_2 &= \dot{\mathbf{X}}_2 - \dot{\mathbf{X}}_2^{\mathrm{ref}} = \mathbf{F}_2(\mathbf{X}_1, \mathbf{X}_2) + \mathbf{B}_2(\mathbf{X}_1)\mathbf{U} + \Delta\mathbf{d}_2 - \mathbf{F}_2(\mathbf{X}_1, \mathbf{X}_2^{\mathrm{ref}}) - \mathbf{B}_2(\mathbf{X}_1)\bar{\mathbf{U}} \\ &= \mathbf{F}_2(\mathbf{X}_1, \mathbf{X}_2^{\mathrm{ref}} + \mathbf{E}_2) + \mathbf{B}_2(\mathbf{X}_1)(\bar{\mathbf{U}} + \tilde{\mathbf{U}}) + \Delta\mathbf{d}_2 - \mathbf{F}_2(\mathbf{X}_1, \mathbf{X}_2^{\mathrm{ref}}) - \mathbf{B}_2(\mathbf{X}_1)\bar{\mathbf{U}}\end{aligned} \tag{18}$$

where $\tilde{\mathbf{U}} = \mathbf{U} - \bar{\mathbf{U}}$. By linearizing (18) along the nominal trajectory ($\mathbf{X}_2^{\mathrm{ref}}$, $\bar{\mathbf{U}}$), it is obtained that

$$\dot{\mathbf{E}}_2 = \mathbf{A}_2(t)\mathbf{E}_2 + \mathbf{B}_2(t)\tilde{\mathbf{U}} + \Delta\mathbf{d}_2 \tag{19}$$

where $\mathbf{A}_2(t)=\left.\dfrac{\partial \mathbf{F}_2(\mathbf{X}_1,\mathbf{X}_2)}{\partial \mathbf{X}_2}\right|_{\mathbf{X}_2^{\text{ref}}}$, $\mathbf{B}_2(t)=\mathbf{B}_2(\mathbf{X}_1)$.

To deal with the tracking error stabilization problem of system (19), a sliding surface is chosen as

$$\boldsymbol{S}=\mathbf{E}_2 \tag{20}$$

Note, the sliding surface has the same dimension with the order of system (19). Therefore, it only needs to consider the reachability issue of the corresponding error dynamics. Now consider the following reaching law

$$\dot{\boldsymbol{S}}=-\boldsymbol{\tau}\boldsymbol{S}-\boldsymbol{\varepsilon}\left|\boldsymbol{S}\right|^{\gamma}\operatorname{sgn}(\boldsymbol{S}) \tag{21}$$

where $\boldsymbol{\tau}=\operatorname{diag}[\tau_1,\tau_2]^T$, $\tau_i>0$, $\boldsymbol{\varepsilon}=\operatorname{diag}[\varepsilon_1,\varepsilon_2]^T$, $\varepsilon_i>0$, $\operatorname{sgn}(\boldsymbol{S})=[\operatorname{sgn}(S_1),\operatorname{sgn}(S_2)]^T$, $\left|\boldsymbol{S}\right|^{\gamma}=\left[\left|S_1\right|^{\gamma},\left|S_2\right|^{\gamma}\right]^T$, $0<\gamma<1$, and S_i is the ith component of $\boldsymbol{S}$. From Eqs. (19) and (20), the derivative of $\boldsymbol{S}$ can be derived as

$$\dot{\boldsymbol{S}}=\dot{\mathbf{E}}_2=\mathbf{A}_2(t)\mathbf{E}_2+\mathbf{B}_2(t)\tilde{\mathbf{U}}+\Delta\mathbf{d}_2 \tag{22}$$

Using the reaching law (21), a pseudo-law is designed as

$$\tilde{\mathbf{U}}_{\text{pseudo}}=\mathbf{B}_2^{-1}\left(-\mathbf{A}_2(t)-\Delta\mathbf{d}_2-\boldsymbol{\tau}\boldsymbol{S}-\boldsymbol{\varepsilon}\left|\boldsymbol{S}\right|^{\gamma}\operatorname{sgn}(\boldsymbol{S})\right) \tag{23}$$

Next, the objective is to estimate the uncertainty $\Delta\mathbf{d}_2$ in (23). Also, an extended state $\mathbf{X}_5$ is introduced as the uncertainty $\Delta\mathbf{d}_2$, the system (3) is rewritten as

$$\begin{cases}\dot{\mathbf{X}}_2=\mathbf{F}_2(\mathbf{X}_1,\mathbf{X}_2)+\mathbf{B}_2(\mathbf{X}_1)\mathbf{U}+\mathbf{X}_5\\ \dot{\mathbf{X}}_5=\xi_2(t)\end{cases} \tag{24}$$

where the function $\xi_2(t)$ is the derivative of the uncertainty $\Delta\mathbf{d}_2$. Then the following second-order ESO [12] for system (24) is applied to estimate the uncertainty $\Delta\mathbf{d}_2$

$$\begin{cases}\dot{\hat{\mathbf{X}}}_2=\hat{\mathbf{X}}_5+l_1\mathbf{e}_2+\mathbf{F}_2(\hat{\mathbf{X}}_1,\hat{\mathbf{X}}_2)+\mathbf{B}_2(\hat{\mathbf{X}}_1)(\bar{\mathbf{U}}+\tilde{\mathbf{U}})\\ \dot{\hat{\mathbf{X}}}_5=l_2\mathbf{e}_2\end{cases} \tag{25}$$

where $\mathbf{e}_2=\mathbf{X}_2-\hat{\mathbf{X}}_2$ is the estimation error of the ESO, $\hat{\mathbf{X}}_2$ is the estimate of $\mathbf{X}_2$, $\hat{\mathbf{X}}_5$ is the estimate of $\mathbf{X}_5$. With the uncertainty estimated by (25), the control law (23) is modified as

$$\tilde{\mathbf{U}}=\mathbf{B}_2^{-1}\left(-\mathbf{A}_2(t)-\hat{\mathbf{X}}_5-\boldsymbol{\tau}\boldsymbol{S}-\boldsymbol{\varepsilon}\left|\boldsymbol{S}\right|^{\gamma}\operatorname{sgn}(\boldsymbol{S})\right) \tag{26}$$

Finally, the overall control law for angular rate loop is

$$\mathbf{U}=\bar{\mathbf{U}}+\tilde{\mathbf{U}} \tag{27}$$

where $\bar{\mathbf{U}}$ and $\tilde{\mathbf{U}}$ are defined in (17) and (26) respectively.

IV. Stability Analisis

In this section, the stability of the closed-loop system of (2) and (3) is analyzed. Before giving the theorem, the following lemmas are needed.

Lemma 1. [14]: If $p\in(0,2)$, then the flowing inequality holds

$$\left(\sum_{i=1}^{2}\left|x_i\right|^2\right)^{p/2}\le\sum_{i=1}^{2}\left|x_i\right|^p \tag{28}$$

Lemma 2. [14]: The equilibrium point x=0 of the system $\dot{x}=f(x)$ is globally finite-time stable for any given condition $x(0)=x_0$, if a Lyapunov description can be obtained as

$$\begin{gathered}\dot{V}(x)+\lambda_1V(x)+\lambda_2V^{\alpha}(x)\le 0\\ \lambda_1>0,\lambda_2>0,0<\alpha<1\end{gathered} \tag{29}$$

and the setting time can be given by

$$T\le\frac{1}{\lambda_1(1-\alpha)}\ln\frac{\lambda_1V^{1-\alpha}(x_0)+\lambda_2}{\lambda_2} \tag{30}$$

Theorem 1. Consider the tracking error dynamics of angular rate loop. The proposed control law (26) together with the ESO described in (25), guarantees that the tracking error trajectory for the angular rate loop is driven onto the sliding surface in finite time and converge to a residual set of the origin.

Proof. Consider the following Lyapunov function candidate

$$V_1=\frac{1}{2}\boldsymbol{S}^T\boldsymbol{S} \tag{31}$$

Taking the derivative of (31) and applying the control (26) to (22) yields

$$\begin{aligned}\dot{V}_1=\boldsymbol{S}^T\dot{\boldsymbol{S}}&=\boldsymbol{S}^T\left(-\boldsymbol{\tau}\boldsymbol{S}-\boldsymbol{\varepsilon}\left|\boldsymbol{S}\right|^{\gamma}\operatorname{sgn}(\boldsymbol{S})+\Delta\mathbf{d}_2-\Delta\hat{\mathbf{d}}_2\right)\\&=-\boldsymbol{\tau}\left\|\boldsymbol{S}\right\|^2-\boldsymbol{\varepsilon}\left\|\boldsymbol{S}\right\|^{\gamma+1}+\boldsymbol{S}^T\Delta\tilde{\mathbf{d}}_2\end{aligned} \tag{32}$$

where $\Delta\tilde{\mathbf{d}}_2$ is the estimate error for $\Delta\mathbf{d}_2$ and $\Delta\tilde{\mathbf{d}}_2=\Delta\mathbf{d}_2-\Delta\hat{\mathbf{d}}_2$. According to Lemma 1, we have

$$\dot{V}_1\le-2\tau_{\min}V_1-\varepsilon_{\min}2^{(\gamma+1)/2}V_1^{(\gamma+1)/2}+\left|\boldsymbol{S}^T\Delta\tilde{\mathbf{d}}_2\right| \tag{33}$$

where $\tau_{\min}=\min(\tau_i)$ and $\varepsilon_{\min}=\min(\varepsilon_i)$. Suppose that there exists a scalar $0<\theta\le1$ such that the inequality (33) can be expressed as

$$\begin{aligned}\dot{V}_1\le&-\left(2\tau_{\min}V_1+\varepsilon_{\min}2^{(\gamma+1)/2}V_1^{(\gamma+1)/2}\right)\theta\\&-\left(2\tau_{\min}V_1+\varepsilon_{\min}2^{(\gamma+1)/2}V_1^{(\gamma+1)/2}\right)(1-\theta)+\left|\boldsymbol{S}^T\Delta\tilde{\mathbf{d}}_2\right|\end{aligned} \tag{34}$$

It is clear that $\dot{V}_1\le-\left(2\tau_{\min}V_1+\varepsilon_{\min}2^{(\gamma+1)/2}V_1^{(\gamma+1)/2}\right)\theta$ if $\left(2\tau_{\min}V_1+\varepsilon_{\min}2^{(\gamma+1)/2}V_1^{(\gamma+1)/2}\right)(1-\theta)\ge\left|\boldsymbol{S}^T\Delta\tilde{\mathbf{d}}_2\right|$. According to Lemma 2, the decrease of $V_1(t)$ eventually drives the trajectory of the closed-loop angular rate tracking error into the set

$$\boldsymbol{S}\in\left(\tau_{\min}\boldsymbol{S}+\varepsilon_{\min}\left|\boldsymbol{S}\right|^{\gamma}\le\frac{\Delta\tilde{\mathbf{d}}_2}{1-\theta}\right) \tag{35}$$

with the reaching time

$$T_{\text{reach}}\le\frac{1}{\tau_{\min}\theta(1-\gamma)}\ln\frac{2\tau_{\min}V^{(1-\gamma)/2}(\boldsymbol{S}(0))+\varepsilon_{\min}2^{(\gamma+1)/2}}{\varepsilon_{\min}2^{(\gamma+1)/2}} \tag{36}$$

It should be noted that the estimate error of ESO is proved to be much smaller by appropriately selection of parameters l_1 and l_2 [13]. Consequently, (35) indicates that the trajectory of the closed-loop angular rate tracking error is bounded by a very small set.

Theorem 2. Consider the tracking error dynamics of attitude loop. The proposed control law (15) together with the ESO described by (14), guarantees that the tracking error for attitude loop converge to a residual set of the origin.

Proof. Consider the following Lyapunov function candidate

$$V_2=\frac{1}{2}\mathbf{E}_1^T\mathbf{E}_1 \tag{37}$$

Taking the derivative of (37) and making use of the control (15) yields

$$\begin{aligned}\dot{V}_2 &= \mathbf{E}_1^T\dot{\mathbf{E}}_1 = \mathbf{E}_1^T\dot{\mathbf{E}}_1 \\ &= \mathbf{E}_1^T\left(\mathbf{A}_1(t)\mathbf{E}_1 + \mathbf{B}_1(t)\tilde{\mathbf{X}}_2 + \Delta\mathbf{d}_1\right) \\ &= \mathbf{E}_1^T\left(-\mathbf{K}_1\mathbf{E}_1 + \Delta\mathbf{d}_1 - \hat{\mathbf{X}}_3\right)\end{aligned} \tag{38}$$

Considering the estimate error of ESO yields

$$\dot{V}_2 = \mathbf{E}_1^T\left(-\mathbf{K}_1\mathbf{E}_1 + \Delta\tilde{\mathbf{d}}_1\right) \le -k_{\min}\|\mathbf{E}_1\|^2 + \|\mathbf{E}_1\|\|\Delta\tilde{\mathbf{d}}_1\| \tag{39}$$

where $k_{\min} = \min(k_i)$ and $\Delta\tilde{\mathbf{d}}_1$ is the estimate error for $\Delta\mathbf{d}_1$. Also, $\Delta\tilde{\mathbf{d}}_1$ is bounded by appropriately selecting parameters l_1 and l_2 as proved in [13]. Thus, when the design parameter k_i is chosen large enough, $\dot{V}_2 < 0$ can be guaranteed. Furthermore, the decrease of V_2 eventually drives the tracking error trajectory of the attitude loop into $\|\mathbf{E}_1\| \le \|\Delta\tilde{\mathbf{d}}_1\| / k_{\min}$ which depends on the error $\Delta\tilde{\mathbf{d}}_1$.

V. Simulation Results

In this section, the effectiveness of the proposed control scheme is evaluated by numerical simulation. Comparison with the existing results is also provided.

The ESO parameters are chosen as l_1=240 and l_2=1920, the bandwidth of the pseudo differentiator is $\omega_d = 50$, the parameters of the controller are $\mathbf{K}_1 = 10\mathbf{I}_2$, $\boldsymbol{\tau} = 5\mathbf{I}_2$, $\boldsymbol{\varepsilon} = 0.4\mathbf{I}_2$ and $\gamma = 0.7$. For simulation purpose, the uncertainties are given by

$$\Delta\mathbf{d}_1=[0.2\sin\alpha+0.1\cos(4t)\ \ 0.1\sin(50\alpha)\cos\beta]^{\mathrm{T}},$$

$$\Delta\mathbf{d}_2=[3.1\sin(2t)\ \ 2.2\sin(t)\cos(2t)]^{\mathrm{T}}.$$

For the purpose of comparison, the traditional TLC proposed in [8] is also applied for the case study. The attitude angle, angular rate and deflection angles obtained by the proposed control scheme are shown in Fig. 3. It is obvious that the closed-loop RAV system can perform a nice tracking property in the presence of uncertainties. As shown in the local time history of the attitude trajectory, the angle of attack can track its reference accurately and rapidly. In addition, the deflection angles are chattering free and fairly smooth. The estimate performance of the ESO is shown in Fig. 4. It is clearly that the ESO can estimate the uncertainties with fast speed and high accuracy. An accurate estimation of uncertainties contributes to a better disturbance rejection and smooth control profile for the closed-loop system. Therefore, an acceptable and feasible tracking performance for RAV can be assured under the proposed control scheme even in the presence of large uncertainties.

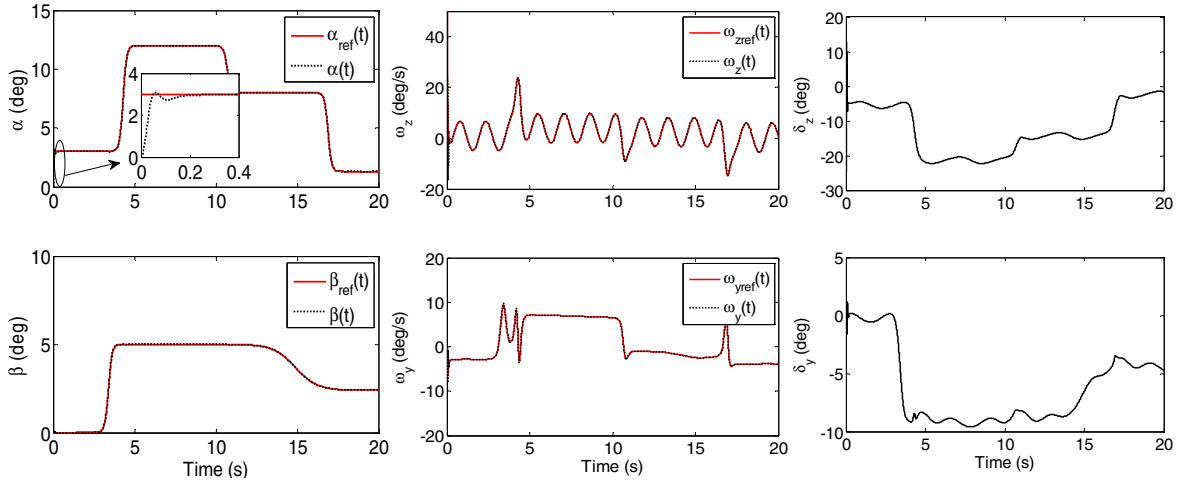

Fig. 3 Simulation results for the proposed control scheme

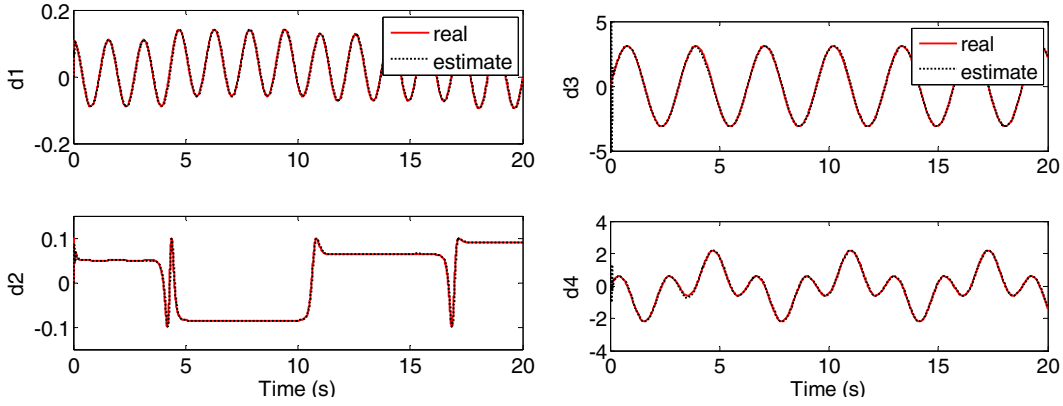

Fig. 4 Estimate performance of ESO

In order to compare with the results in [8], simulations on TLC have been carried out using the same parameters. The time histories of attitude angle, angular rate and deflection angle are shown in Fig. 5. It can be observed that the tracking performance of TLC degrades remarkably as compared with that of the proposed method. The attitude angles only track its command roughly, and severe oscillations can also be observed in the corresponding time response. Moreover, the tracking performance of angular rate is with obvious tracking error during the entire flight. Because TLC in [8] does not contain any observers to tackle the uncertainties, so this method cannot exhibit a good uncertainty rejection as stated above.

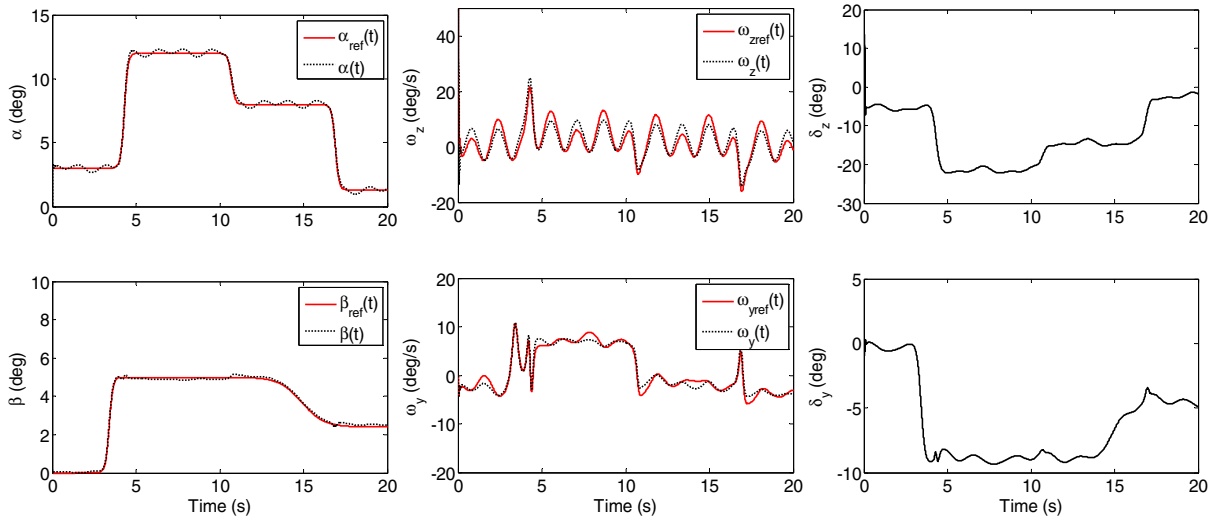

Fig. 5 Simulation results for TLC

VI. Conclusion

In this paper, the attitude control problem for a RAV which is a highly coupled nonlinear system, has been investigated. A novel control scheme integrated the philosophy of TLC and the observer-based variable structure control into a backstepping control procedure is presented. The ESO is applied to estimate uncertainties, and the stability of the corresponding closed-loop system is obtained based on Lyapunov theory. Simulation results are presented to demonstrate the effectiveness and feasibility of the proposed control scheme. Comparisons with the traditional TLC have also been carried out to show the advantages of the proposed method.

References

[1] R. Lestage. "Analysis of control and guidance of rolling missiles with a single plane of control fins," AIAA Guidance, Navigation, and Control Conference and Exhibit. Denver: AIAA. 2000: 14-17.

[2] Y. Koohmaskan, R. A. Arvan, A. R. Vali, et al. "Dynamic stability conditions for a rolling flight vehicle applying continuous actuator." Aerospace Science and Technology, 2015, 42: 451-458.

[3] B. E. Jun. "An effective integral control law for rolling airframe missiles with a single plane of control surfaces," 2013 13th International Conference on Control, Automation and Systems. IEEE, 2013: 66-71.

[4] H. S. Ju, C. C. Tsai. "Longitudinal axis flight control law design by adaptive backstepping," IEEE Transactions on Aerospace and Electronic Systems, 2007, 43(1): 311-329.

[5] J. T. Parker, A. Serrani, S. Yurkovich, et al, "Control-orientedmodeling of an air-breathing hypersonic vehicle," Journal of Guidance, Control, and Dynamics, 2007, 30(3): 856–869.

[6] O.U. Rehman, B. Fidan, and I. Petersen, "Minimax LQR control design for a hypersonic flight vehicle," in Proceedings of the 16th AIAA/DLR/DGLR International Space Planes and Hypersonic Systems and Technologies Conference, AIAA-2010–8285, October 2009.

[7] O. U. Rehman, I. R. Petersen, and B. Fidan, "Robust nonlinear control of a nonlinear uncertain system with input coupling and its application to hypersonic flight vehicles," in Proceedings of the IEEE International Conference on Control Applications, Yokohama, Japan, September 2010: 1451–1457.

[8] J. Zhu, A. S. Hodel, and K. Funston. "X-33 ascent flight control design by trajectory linearization – a sigular perturbation approach," AIAA Guidance, Navigation, and Control Conference and Exhibit. Denver: AIAA. 2000: 1-19.

[9] X. Shao, and H. Wang. "Active disturbance rejection based trajectory linearization control for hypersonic reentry vehicle with bounded uncertainties," ISA Transactions, 2015, 54: 27-38.

[10] J. Zhu, C. Jiang, and Y. Xue. "Robust adaptive trajectory linearization control for aerospace vehicle using single hidden layer neutral networks," Acta Armamentarii, 2008, 29(1): 52-56.

[11] X. Qian, R. Lin, and Y. Zhao. Missile flight mechanics, Beijing: Beijing Institute Technology Press, 2008.

[12] Jingqing Han. "From PID to active disturbance rejection control," IEEE Transaction on industrial electronics, 2009, 56(3): 900-906.

[13] Q. Zheng, L. Q. Gao, and Z. Gao. "On validation of extended state observer through analysis and experimentation," Journal of Dynamic Systems, Measurement, and Control, 2012, 134(2): 024505.

[14] X. G. Yan and S. Zhang. "Design of Robust Controllers with Similar Structure for Nonlinear Uncertain Composite Large-Scale Systems Possessing Similarity". Control Theory and Applications, 1997, 14(4): 513-519.

[15] X. G. Yan, S. K. Spurgeon and C. Edwards. "Memoryless static output feedback sliding mode control for nonlinear systems with delayed disturbances," IEEE Transaction on Automatic Control, 2014, 59(7): 1906-1912.

[16] X. G. Yan, S. K. Spurgeon and C. Edwards. "On discontinuous static output feedback control for linear systems with nonlinear disturbances," Systems & Control Letters, 2009, 58(5): 314-319.